Inorganic Chemistry

ARTICLE

pubs.acs.org/IC

Phase-Selective Synthesis of Nickel Phosphide in High-Boiling Solvent for All-Solid-State Lithium Secondary Batteries

Keigo Aso, Akitoshi Hayashi, and Masahiro Tatsumisago*

Department of Applied Chemistry, Graduate School of Engineering, Osaka Prefecture University, 1-1 Gakuen-cho, Naka-ku, Sakai, Osaka 599-8531, Japan

ABSTRACT: Nickel phosphide particles were synthesized by thermal decomposition of a nickel precursor in a mixed solution of trioctylphosphine and trioctylphosphine oxide. The crystal phase and morphology of samples prepared by changing the solvents, the amount of trioctylphosphine as a phosphorus source, the reaction temperature, and the nickel precursor were characterized using X-ray diffraction and transmission electron microscopy. Spherical Ni_5P_4 particles with diameters of 500 nm were obtained using nickel acetylacetonate as a nickel precursor at 360 °C for 1 h in trioctylphosphine oxide. NiP_2 particles with diameters of 200−500 nm were obtained using nickel acetate tetrahydrate at 360 °C for 5 h in trioctylphosphine oxide. All-solid-state cells were fabricated using NiP_2 particles as an active material and $80Li_2S \cdot 20P_2S_5$ (mol %) glass−ceramic as a solid electrolyte. The Li−In/$80Li_2S \cdot 20P_2S_5$/NiP_2 cell exhibited an initial discharge capacity of 1100 mAh g^{-1} at a current density of 0.13 mA cm^{-2} and retained a discharge capacity of 750 mAh g^{-1} after 10 cycles.

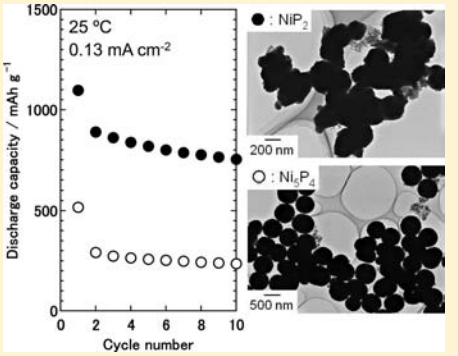

1. INTRODUCTION

Lithium-ion batteries are used as power sources for a wide range of portable devices due to their high operating voltage, high energy density, lightweight, and longer cycle life.[1] Large-sized lithium-ion batteries with high safety characteristics are presently in demand for application as power sources in plug-in hybrid and electric vehicles. All-solid-state lithium secondary batteries that employ inorganic solid electrolytes have attracted much attention, because these batteries are extremely safe, reliable, and free from electrolyte leakage, as is problematic with liquid electrolytes.[2] Much effort has been directed to develop the solid electrolytes with high lithium-ion conductivity. Among many kinds of solid electrolyte, sulfide-based solid electrolytes are promising because of high lithium-ion conductivities at room temperature. Sulfide glasses in the systems Li_2S-SiS_2 and $Li_2S-P_2S_5$ prepared by the melt-quenching method are known as lithium-ion conductors with high conductivities over 10^{-4} S cm^{-1} at room temperature.[3−6] Kanno et al. found that the sulfide crystalline lithium superionic conductor, thio-LISICON (such as solid solutions in the system $Li_4GeS_4-Li_3PS_4$), exhibited a high lithium-ion conductivity of $10^{-7}-10^{-3}$ S cm^{-1} at room temperature.[7] On the other hand, we reported that crystallization of $Li_2S-P_2S_5$ glasses prepared by a mechanical milling technique improved their conductivities.[8,9] $Li_2S-P_2S_5$ glass−ceramic electrolytes with a high lithium-ion conductivity of 5×10^{-3} S cm^{-1} at room temperature, which is close to that of organic liquid electrolytes, are some of the most promising electrolytes for all-solid-state cells.[10]

We reported the electrochemical performance of all-solid-state cells using $Li_2S-P_2S_5$ glass−ceramic solid electrolytes. For example, the all-solid-state cells using $LiCoO_2$ and $Li_4Ti_5O_{12}$ as an active material exhibited high capacities and excellent cycle performance during 500 and 700 cycles at room temperature.[11] The all-solid-state cells using sulfur active material with the large theoretical capacity of 1672 mAh g^{-1} exhibited excellent cycle performance for 200 cycles, while Li/S batteries using organic liquid electrolytes were reported to suffer from a rapid capacity fading during cycling because of dissolution of soluble lithium polysulfides into liquid electrolytes.[12] In addition, development of all-solid-state batteries has stimulated research on active materials with high capacity and high rate capability.[13−15] We reported the synthesis of monodispersed α-Fe_2O_3 particles of various sizes by a solution process using aqueous NaOH solution; an all-solid-state cell fabricated using an electrode prepared with submicrometer-size α-Fe_2O_3 particles exhibited a higher capacity than a cell using micrometer-size α-Fe_2O_3 particles for the electrode.[16] Composite electrodes composed of active materials, solid electrolytes (lithium-ion conduction path), and conductive additives (electron conduction path) are often employed in bulk-type all-solid-state cells. Electrochemical reactions proceed at the solid−solid interface and are affected by the contact states of the interfaces in the composite electrode. It is expected that the contact area among constituents in composite electrodes is increased with decreasing the particle size of monodispersed active materials.

Metal phosphides have been applied as an active material in lithium-ion batteries that employ organic liquid electrolytes.[17] Metal phosphide electrodes exhibit lower intercalation potentials

Received: June 27, 2011
Published: October 03, 2011

dx.doi.org/10.1021/ic2013733 | *Inorg. Chem.* 2011, 50, 10820–10824

and larger capacities compared to the corresponding metal oxides and sulfides and are expected to be a promising alternative to graphite negative electrode materials. Nickel phosphide electrodes such as Ni_3P, NiP_2, and NiP_3 have been applied as active materials in cells using liquid electrolytes.[18−20] Ni_3P electrodeposited onto Ni foam had a capacity of 400 mAh g^{-1} after 20 cycles.[18] NiP_3 exhibited a first discharge capacity of 1475 mAh g^{-1}; however, capacity fade was observed within the first 10 cycles.[19] On the other hand, it was reported that NiP_2 had a relatively high capacity (1000−1300 mAh g^{-1}) and good cycle performance in a cell using a liquid electrolyte.[20] We also reported that all-solid-state cells using micrometer-size NiP_2 particles prepared by a mechanical milling technique from nickel metal and red phosphorus powders exhibited high reversible capacity (over 600 mAh g^{-1}) for 10 cycles at room temperature.[21]

Nanomaterials prepared by a solution process using high-boiling solvents have attracted attention.[22] It was reported that various metal phosphides, such as MnP, Co_2P, FeP, and Ni_2P, and sulfides, such as Cu_2S, ZnS, MnS, and PbS, were synthesized using this process.[23,24] In addition, this process is a facile route to synthesize nanoparticles with uniform size and various morphologies. The size and morphology of the obtained particles can be varied using different coordinating solvents.[22,25] Nanoparticles prepared by the solution process using high-boiling solvents have been applied as active materials to lithium-ion batteries using conventional liquid electrolytes.[26−28] We also reported that NiS or $SnP_{0.94}$ active materials prepared using high-boiling solvents exhibited high capacity in all-solid-state cells.[29,30] An all-solid-state cell using solution-derived NiS nanoparticles (50 nm diameter) exhibited a larger capacity than that using NiS particles prepared by mechanical milling from nickel metal and elemental sulfur powders.[29] The mechanical milling process is appropriate to large-scale synthesis; however, the particles obtained via this process tend to be nonuniform in size and prone to aggregation.

The capacity of all-solid-state cells is expected to increase with decreasing the size of uniformly sized NiP_2 particles. Wang et al. reported the synthesis of hollow nickel phosphide (mixed phase of Ni_2P and $Ni_{12}P_5$) nanoparticles using nickel acetylacetonate ($Ni(acac)_2$; nickel precursor) and trioctylphosphine (TOP; ligand and phosphorus source).[31] Barry et al. reported the synthesis of 50−100 nm sized NiP_2 particles under anhydrous solvothermal reaction conditions in a stainless steel autoclave using nickel chloride as a nickel precursor with yellow molecular P_4 as a phosphorus source.[32]

In this study, NiP_2 particles were first synthesized in high-boiling solvents at ambient pressure. The crystal phase of nickel phosphide was controlled by selection of the nickel precursors. The NiP_2 particles obtained were applied as the active material in all-solid-state cells with $Li_2S−P_2S_5$ solid electrolytes. The electrochemical properties of the cells were investigated by charge−discharge measurements.

2. EXPERIMENTAL SECTION

Nickel(II) acetylacetonate ($Ni(acac)_2$; 0.385 g, 1.5×10^{-3} mol) was mixed with trioctylphosphine (TOP; 10 mL, 2.2×10^{-2} mol) as a phosphorus source and trioctylphosphine oxide (TOPO; 2.5 g, 6.5×10^{-3} mol) as a coordinating solvent in a 200 mL four-necked flask. The mixture in the flask was heated to 360 °C and refluxed for 1 h in an Ar atmosphere. This is referred to as the "original condition" throughout. After heating, the mixture was cooled to room temperature and subsequently washed with hexane and ethanol. The resultant particles were isolated by centrifuging the mixture and then removing the supernatants. The obtained powder was dried in a vacuum oven at 120 °C for 6 h. The following four parameters were investigated for control of the crystal phase of the nickel phosphide particles: the use of docosane (DCS; $CH_3(CH_2)_{20}CH_3$, 2.5 g) as a noncoordinating solvent, the amount of TOP, the reaction temperature, and the type of nickel precursor used, such as nickel acetylacetonate dihydrate ($Ni(acac)_2 \cdot 2H_2O$) and nickel acetate tetrahydrate ($Ni(Ac)_2 \cdot 4H_2O$).

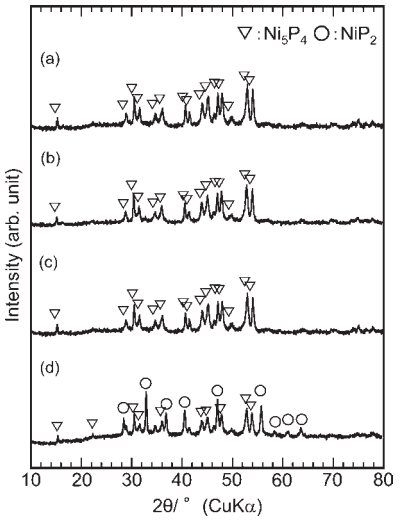

Figure 1. XRD patterns of samples prepared (a) using the "original condition" (reflux with TOPO at 360 °C for 1 h), (b) using DCS instead of TOPO, (c) changing the amount of TOP, or (d) refluxing at 360 °C for 5 h.

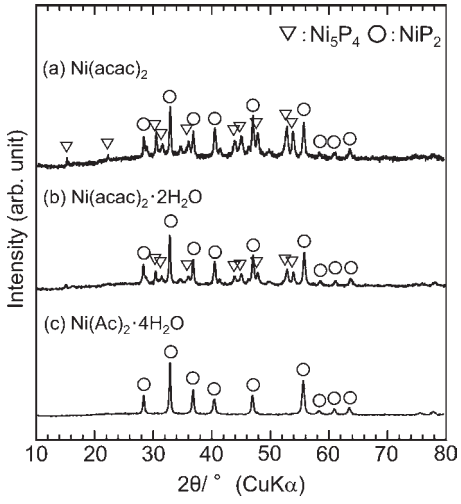

Figure 2. XRD patterns of samples prepared by refluxing (a) $Ni(acac)_2$, (b) $Ni(acac)_2 \cdot 2H_2O$, or (c) $Ni(Ac)_2 \cdot 4H_2O$ in TOPO at 360 °C for 5 h.

X-ray diffraction (XRD; UltimaIV; Rigaku) measurements were performed using Cu Kα radiation to identify the crystalline phases. The morphology of the particles obtained was investigated using transmission electron microscopy (TEM; JEM-2000FX; JEOL).

Laboratory-scale solid-state cells were fabricated as follows. The $80Li_2S \cdot 20P_2S_5$ (mol %) glass−ceramic solid electrolyte was prepared by mechanical milling and subsequent heat treatment of a mixture of Li_2S and P_2S_5, which exhibited a wide electrochemical window and a high ionic conductivity at room temperature.[10] A composite electrode

dx.doi.org/10.1021/ic2013733 |Inorg. Chem. 2011, 50, 10820–10824

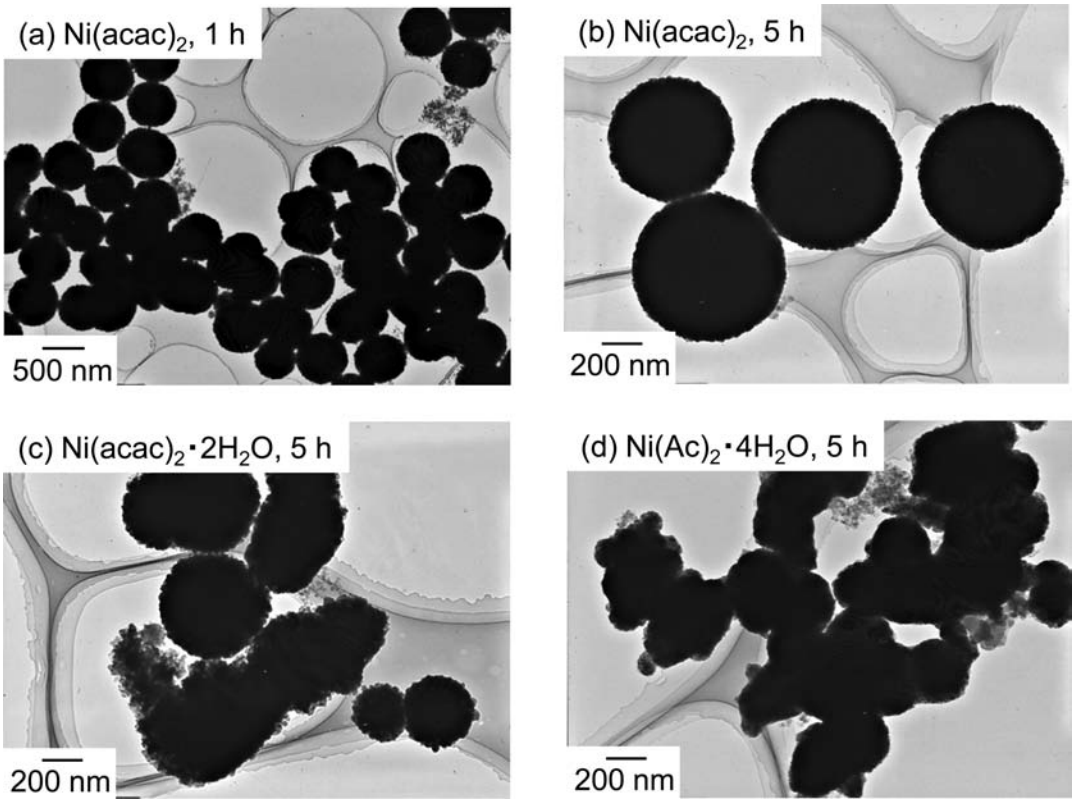

Figure 3. TEM images of samples prepared by refluxing (a, b) $Ni(acac)_2$, (c) $Ni(acac)_2 \cdot 2H_2O$, or (d) $Ni(Ac)_2 \cdot 4H_2O$ in TOPO at 360 °C. The reaction time was 1 h for (a) and 5 h for (b, c, and d).

material was prepared by hand grinding a mixture of the nickel phosphide active material (5.7 mg), the glass−ceramic electrolyte (8.5 mg), and vapor grown carbon fiber (VGCF) as a conductive additive (0.8 mg). Two-electrode cells were fabricated using the nickel phosphide composite electrode as a working electrode, the glass−ceramic electrolyte, and a Li−In alloy as a counter electrode. The working electrode and solid electrolyte were placed in a polycarbonate tube (10 mm diameter) and pressed together under 360 MPa at room temperature. Li−In alloy was placed on the surface of the solid electrolyte side of the bilayer pellet, and a pressure of 120 MPa was then applied to give a three-layered pellet. The three-layered pellet was finally sandwiched with two stainless-steel disks as current collectors. All cell preparation processes were carried out in a dry Ar-filled glovebox. Electrochemical tests were conducted under a constant current density of 0.13 mA cm^{-2} at 25 °C in an Ar atmosphere using a charge−discharge measurement device (BTS-2004, Nagano Co.).

3. RESULTS AND DISCUSSION

Figure 1 shows the XRD patterns of samples prepared using various parameters. Figure 1a shows the XRD pattern of the sample prepared under the "original condition". The sample was identified as Ni_5P_4 (JCPDS #018-0883). The effect of the reaction conditions on the crystal phase of the obtained nickel phosphide particles was investigated. We previously reported that the crystal phase of nickel sulfide particles was changed from Ni_9S_8 to NiS when using a noncoordinating solvent.[29] In this study, DCS was used as a noncoordinating solvent. Wang et al. reported that the phase control of cobalt phosphide was achieved by changing the ratio of metal to TOP (phosphorus source) and the reaction time.[33] In the present study, the amount of TOP as a phosphorus source was increased from 10 (2.2×10^{-2} mol) to 20 mL (4.4×10^{-2} mol) and the reaction time was increased from 1 to 5 h. Figure 1b and 1c shows the XRD patterns of the samples prepared using DCS as a noncoordinating solvent and with an increased amount of TOP, respectively. The crystal phase of both samples was still Ni_5P_4. The sample obtained by heating for 5 h (Figure 1d) was a mixture of Ni_5P_4 and NiP_2 (JCPDS #021-0590), which suggests that Ni_5P_4 particles are generated first by thermal decomposition of nickel acetylacetonate in TOP and then NiP_2 particles are formed by further diffusion of phosphorus derived from TOP into Ni_5P_4.

Figure 2 shows the XRD patterns of the samples prepared by changing the nickel precursors. Figure 2a and 2b shows XRD patterns of samples prepared using $Ni(acac)_2$ and $Ni(acac)_2 \cdot 2H_2O$, respectively. Both samples were a mixture of Ni_5P_4 and NiP_2. The relative peak intensity of NiP_2 in the sample prepared using $Ni(acac)_2 \cdot 2H_2O$ was stronger than that prepared using $Ni(acac)_2$. In contrast, NiP_2 was obtained as a single phase using $Ni(Ac)_2 \cdot 4H_2O$, as shown in Figure 2c. In the crystal structure of $Ni(Ac)_2 \cdot 4H_2O$, nickel atoms are surrounded by four water molecules and two oxygen atoms which belong to two different acetate groups.[34,35] Silva et al. reported that cobalt nanoparticles were synthesized using acetylene-bridged dicobalt hexacarbonyl (starting material) and TOP (surfactant); the lone pair of the phosphorus atom in TOP could easily coordinate to cobalt atoms in acetylene-bridged dicobalt hexacarbonyl.[36] In our case, TOP molecules as a phosphorus source could possibly substitute for water molecules in the structure of $Ni(Ac)_2 \cdot 4H_2O$, and therefore, $Ni(Ac)_2 \cdot 4H_2O$ could promote diffusion of phosphorus derived from TOP to nickel atoms.

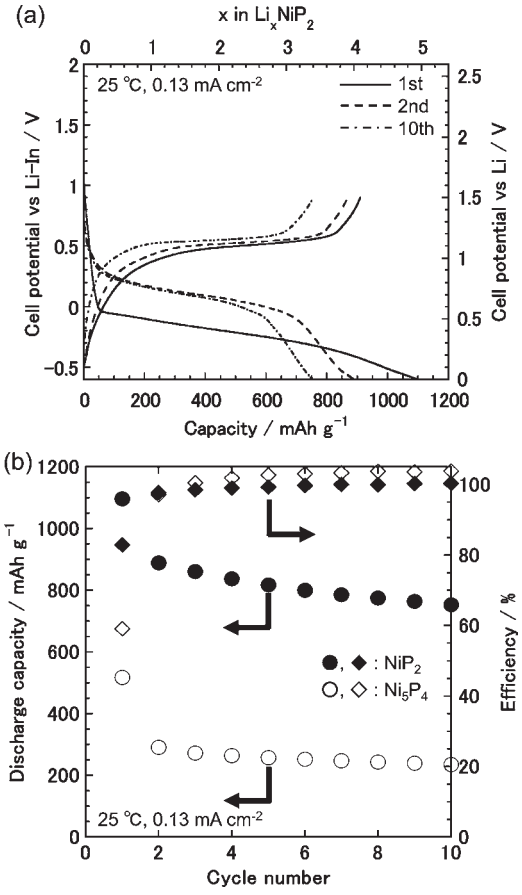

Figure 4. (a) Charge−discharge curves of the Li−In/80Li_2S·20P_2S_5/NiP_2 all-solid-state cell. (b) Cycle performance for all-solid-state cells using NiP_2 or Ni_5P_4 particles.

Figure 3 shows TEM images of the sample prepared by the "original condition" and by changing the nickel precursor. The crystal phases of the prepared samples were identified by XRD measurements as shown in Figures 1 and 2. Spherical Ni_5P_4 particles with diameters of 500 nm were obtained under the "original condition" (Figures 1a and 3a). The particle size of the mixture of Ni_5P_4 and NiP_2 prepared using Ni(acac)$_2$ and heating for 5 h (Figures 2a and 3b) was not different from that prepared under the "original condition". However, the morphologies of the mixture of Ni_5P_4 and NiP_2 prepared using Ni(acac)$_2$·2H_2O (Figures 2b and 3c) and the NiP_2 phase prepared using Ni(Ac)$_2$·4H_2O (Figures 2c and 3d) were not uniform, and their particle sizes were in the range of 200−500 nm.

The 200−500 nm NiP_2 particles prepared using Ni(Ac)$_2$·4H_2O were used to prepare the composite electrode for the all-solid-state cell. Figure 4a shows charge−discharge curves of the Li−In/80Li_2S·20P_2S_5/NiP_2 all-solid-state cell. The cutoff voltages are −0.6 and 0.9 V (vs Li−In). Li−In alloy was used as a counter electrode, because Li−In alloy exhibits a stable potential plateau at 0.62 V vs Li^+/Li, as observed in all-solid-state cells with solid sulfide electrolytes.[37] In Figure 4a, the right-side ordinate axis represents the electrode potential vs Li, which was calculated on the basis of the potential difference between Li−In and Li electrodes (0.62 V). The cell had an initial discharge capacity of 1100 mAh g^{-1} in the voltage range from 0 to 4.0 V (vs Li) under a constant current density of 0.13 mA cm^{-2} at 25 °C. In addition, we reported that the all-solid-state cell using NiP_2 prepared by a mechanical milling technique underwent a conversion process, as also reported in the cells using liquid electrolytes.[21] This conversion process involves the change of NiP_2 to Ni and Li_3P after lithium-ion insertion:[20]

$$NiP_2 + 6Li^+ + 6e^- \rightleftarrows Ni + 2Li_3P$$

The charge−discharge profiles of the all-solid-state cell shown in Figure 4a are similar to those for NiP_2 prepared by mechanical milling. Therefore, 200−500 nm NiP_2 particles prepared by the solution process would also undergo the conversion process. Figure 4b shows the cycle performance for all-solid-state cells using NiP_2 or Ni_5P_4 particles under a constant current density of 0.13 mA cm^{-2} at 25 °C. Ni_5P_4 particles prepared under the "original condition" were used as the active material. The cell using NiP_2 particles exhibited a larger capacity than the cell using Ni_5P_4 particles over 10 cycles. It was reported that an all-solid-state cell using micrometer-size NiP_2 particles exhibited an initial discharge capacity of 1100 mAh g^{-1} at a current density of 0.064 mA cm^{-2}.[21] In this study, the all-solid-state cell with 200−500 nm NiP_2 particles exhibited a capacity of 1100 mAh g^{-1}, even at a higher current density of 0.13 mA cm^{-2}. The high capacity for the all-solid-state cell using submicrometer-size NiP_2 particles is attributable to the decrease in particle size. The cell using submicrometer-size NiP_2 particles retained a discharge capacity of 750 mAh g^{-1} and a charge−discharge efficiency of approximately 100% after 10 cycles, which suggests that submicrometer-size NiP_2 particles prepared in high-boiling solvents are preferable as an active material for all-solid-state batteries.

4. CONCLUSIONS

Nickel phosphide particles were synthesized using high-boiling solvents. Ni_5P_4 particles (500 nm) were obtained by thermal decomposition of Ni(acac)$_2$ as a nickel precursor in a mixed solution of TOP and TOPO at 360 °C for 1 h. The crystal phase of the obtained particles changed from Ni_5P_4 to NiP_2 by increasing the reaction time and using hydrate nickel precursors such as Ni(acac)$_2$·2H_2O and Ni(Ac)$_2$·4H_2O. NiP_2 particles with diameters of 200−500 nm were obtained by thermal decomposition of Ni(Ac)$_2$·4H_2O as a nickel precursor in a mixed solution of TOP and TOPO at 360 °C for 5 h. An all-solid-state cell was fabricated using NiP_2 particles (200−500 nm) as an active material. The Li−In/80Li_2S·20P_2S_5/NiP_2 cell exhibited an initial discharge capacity of 1100 mAh g^{-1} at 0.13 mA cm^{-2} and retained a discharge capacity of 750 mAh g^{-1} after 10 cycles.

AUTHOR INFORMATION

Corresponding Author

*Phone: +81-72-254-9331. Fax: +81-72-254-9331. E-mail : tatsu@chem.osakafu-u.ac.jp.

ACKNOWLEDGMENT

This research was financially supported by the Japan Science and Technology Agency (JST), Core Research for Evolutional Science and Technology (CREST) project. K.A. is thankful for a Grant-in-Aid from the Japan Society for the Promotion of Science (JSPS) Fellows.

REFERENCES

(1) Tarascon, J. M.; Armand, M. *Nature* **2001**, *414*, 359.
(2) Fergus, J. W. *J. Power Sources* **2010**, *195*, 4554.
(3) Mercier, R.; Malugani, J.-P.; Fahys, B.; Robert, G. *Solid State Ionics* **1981**, *5*, 663.
(4) Pradel, A.; Ribes, M. *Solid State Ionics* **1986**, *18/19*, 351.
(5) Kennedy, J. H. *Mater. Chem. Phys.* **1989**, *23*, 29.
(6) Minami, T.; Hayashi, A.; Tatsumisago, M. *Solid State Ionics* **2000**, *136*−*137*, 1015.
(7) Kanno, R.; Murayama, M. *J. Electrochem. Soc.* **2001**, *148*, A742.
(8) Hayashi, A.; Hama, S.; Morimoto, H.; Tatsumisago, M.; Minami, T. *Chem. Lett.* **2001**, 872.
(9) Tatsumisago, M.; Hama, S.; Hayashi, A.; Morimoto, H.; Minami, T. *Solid State Ionics* **2002**, *154*−*155*, 635.
(10) Hayashi, A.; Minami, K.; Ujiie, S.; Tatsumisago, M. *J. Non-Cryst. Solids* **2010**, *356*, 2670.
(11) Tatsumisago, M.; Hayashi, A. *Funct. Mater. Lett.* **2008**, *1*, 31.
(12) Nagao, M.; Hayashi, A.; Tatsumisago, M. *Electrochim. Acta* **2011**, *56*, 6055.
(13) Nagao, M.; Kitaura, H.; Hayashi, A.; Tatsumisago, M. *J. Power Sources* **2009**, *189*, 672.
(14) Nishio, Y.; Kitaura, H.; Hayashi, A.; Tatsumisago, M. *J. Power Sources* **2009**, *189*, 629.
(15) Hayashi, A.; Nishio, Y.; Kitaura, H.; Tatsumisago, M. *Electrochem. Commun.* **2008**, *10*, 1860.
(16) Kitaura, H.; Takahashi, K.; Mizuno, F.; Hayashi, A.; Tadanaga, K.; Tatsumisago, M. *J. Electrochem. Soc.* **2007**, *154*, A725.
(17) Cabana, J.; Monconduit, L.; Larcher, D.; Palacín, M. R. *Adv. Mater.* **2010**, *22*, E170.
(18) Xiang, J. Y.; Tu, J. P.; Wang, X. L.; Huang, X. H.; Yuan, Y. F.; Xia, X. H.; Zeng, Z. Y. *J. Power Sources* **2008**, *185*, 519.
(19) Boyanov, S.; Gillot, F.; Monconduit, L. *Ionics* **2008**, *14*, 125.
(20) Gillot, F.; Boyanov, S.; Dupont, L.; Doublet, M. L.; Morcrette, M.; Monconduit, L.; Tarascon, J. M. *Chem. Mater.* **2005**, *17*, 6327.
(21) Hayashi, A.; Inoue, A.; Tatsumisago, M. *J. Power Sources* **2009**, *189*, 669.
(22) Park, J.; Joo, J.; Soon, G. K.; Jang, Y.; Hyeon, T. *Angew. Chem., Int. Ed.* **2007**, *46*, 4630.
(23) Park, J.; Koo, B.; Yoon, K. Y.; Hwang, Y.; Kang, M.; Park, J.-G.; Hyeon, T. *J. Am. Chem. Soc.* **2005**, *127*, 8433.
(24) Choi, S.-H.; An, K.; Kim, E.-G.; Yu, J. H.; Kim, J. H.; Hyeon, T. *Adv. Funct. Mater.* **2009**, *19*, 1645.
(25) Andelman, T.; Gong, Y.; Polking, M.; Yin, M.; Kuskovsky, I.; Neumark, G.; O'Brien, S. *J. Phys. Chem. B* **2005**, *109*, 14314.
(26) Wang, D. S.; Xie, T.; Peng, Q.; Zhang, S. Y.; Chen, J.; Li, Y. D. *Chem.—Eur. J.* **2008**, *14*, 2507.
(27) Seo, J.-W.; Jang, J.-T.; Park, S.-W.; Kim, C.; Park, B.; Cheon, J. *Adv. Mater.* **2008**, *20*, 4269.
(28) Kim, Y.; Hwang, H.; Yoon, C. S.; Kim, M. G.; Cho, J. *Adv. Mater.* **2007**, *19*, 92.
(29) Aso, K.; Kitaura, H.; Hayashi, A.; Tatsumisago, M. *J. Mater. Chem.* **2011**, *21*, 2987.
(30) Aso, K.; Kitaura, H.; Hayashi, A.; Tatsumisago, M. *J. Ceram. Soc. Jpn.* **2010**, *118*, 620.
(31) Wang, J.; Johnston-Peck, A. C.; Tracy, J. B. *Chem. Mater.* **2009**, *21*, 4462.
(32) Barry, B. M.; Gillan, E. G. *Chem. Mater.* **2008**, *20*, 2618.
(33) Wang, J.; Yang, Q.; Zhang, Z.; Sun, S. *Chem.—Eur. J.* **2010**, *16*, 7916.
(34) Van Niekerk, J. N.; Schoening, F. R. L. *Acta Crystallogr.* **1953**, *6*, 609.
(35) Nicolai, B.; Kearley, G. J.; Johnson, M. R.; Fillaux, F.; Suard, E. *J. Chem. Phys.* **1998**, *109*, 9062.
(36) De Silva, R. M.; Palshin, V.; De Nalin Silva, K. M.; Henry, L. L.; Kumar, C. S. S. R. *J. Mater. Chem.* **2008**, *18*, 738.
(37) Takada, K.; Aotani, N.; Iwamoto, K.; Kondo, S. *Solid State Ionics* **1996**, *86*, 877.